Oceanological and Hydrobiological Studies

International Journal of Oceanography and Hydrobiology

Volume 55, No. 1 March 2026
pages (13-27)

ISSN 1730-413X
eISSN 1897-3191

Halogen and oxyanion variability in marine algae: A study in the St. Martin's Island, Bangladesh

by

Swachsa Rahman[1], Arnob Ghosh[1], Md. Biplob Hasan[1], Moniruzzaman Khondker[2], Fateeha Noor[3], Mir Shariful Islam[1], Mustafizur Rahman Naim[4], Mahmudul Hasan[1,*]

DOI: **https://doi.org/10.26881/oahs-2026.1.02**
Category: **Original research paper**
Received: **September 03, 2025**
Accepted: **December 19, 2025**

[1]*Department of Oceanography, University of Dhaka, Dhaka 1000, Bangladesh*

[2]*Department of Botany, University of Dhaka, Dhaka 1000, Bangladesh*

[3]*Department of Environmental Science, Bangladesh University of Professionals (BUP), Dhaka 1216, Bangladesh*

[4]*Biomedical and Toxicological Research Institute (BTRI), Bangladesh Council of Scientific and Industrial Research (BCSIR), Dhaka, Bangladesh*

* Corresponding author: *mahmud.hasan@du.ac.bd*

Abstract

Halogens and oxyanions play essential roles in marine biogeochemical cycles, yet studies on their distribution in algae remain extremely limited. This work provides the first baseline profile of these ions in the macro- and microalgae of St. Martin's Island, Bangladesh. Eight species representing *Chlorophyta*, *Phaeophyta*, *Rhodophyta*, and *Cyanophyta* were collected during the post-monsoon period, when algal abundance is highest. Anion measurements were carried out using Ion chromatography. Chloride and sulfate were consistently present across all species, with chloride ranging from 3.83 mg · g^{-1} to 23.94 mg · g^{-1} and reaching its highest level in *Ceramium fastigiatum*, while sulfate ranged from 2.88 mg · g^{-1} to 21.35 mg · g^{-1} and peaked in *Padina tenuis*. Fluoride was generally below detection except in *Lyngbya confervoides* (0.10 mg · g^{-1}) and two red macroalgae, including *Hypnea boergesenii* (3.83 mg · g^{-1}). Nitrate accumulation varied among species, with *L. confervoides* showing the lowest level (0.06 mg · g^{-1}) and *Cladophora echinus* the highest (0.32 mg · g^{-1}). As an exploratory dataset, the study documents only the post-monsoon ion patterns and does not capture seasonal or fine-scale spatial variability. Even within this scope, the findings fill a critical regional gap and offer an initial biochemical reference for future ecological assessments and environmental monitoring programs around St. Martin's Island.

Key words: halogen, oxyanions, St. Martin's Island, macroalgae, microalgae

1. Introduction

Marine and coastal ecosystems are hotspots for global biogeochemical cycles, influencing both the local and global scales (Joye et al., 2022). They are interactive systems that incorporate humans together with biological and non-biological components (Woodroffe et al., 2023). In recent years, alterations in marine environments have been observed due to anthropogenic mismanaged activities and climate change, including the distribution and diversity of aquatic organisms, including seaweeds and microalgae (Trégarot et al., 2024). Marine algae absorb important inorganic ions, including halogens and oxyanions that drive biogeochemical cycles and indicate environmental changes like pollution, nutrient cycling, and seawater chemistry. Additionally, regional climate patterns can be influenced by the halogen released from algal cells (Rondan et al., 2024a, 2024b), and their interaction with oxyanions can impact the health of marine water bodies (Lan et al., 2024). Moreover, algal physiology, especially cellular osmoregulation, metabolic processes, and ecological interactions, is impacted by these anions (Al-Adilah et al., 2022; Chen et al., 2023; Giordano et al., 2008). Algal proximate compositions and bioactive compound synthesis are directly linked to those bioaccumulated elements, including halogens and oxyanions, present in high concentrations in seawater (Al-Adila et al., 2020; Küpper et al., 2013). These metabolic characteristics, coupled with the environmental interplay, make algae a bioindicator for marine ecological changes and pollution.

Marine algae have a well-known halogen profile, with a realistic picture of this topic in other regions elsewhere. A multi-technique analysis (Rondan et al., 2024a) and a novel single analytical technique were developed and were successful in assessing macroalgal halogen and sulfur in Antarctic regions (Rondan et al., 2024b). Romarís-Hortas et al. (2012) determined the macroalgal iodine and bromine bioavailability on the Galician coast (northwestern Spain). Edible seaweeds in Greenland were found to bioaccumulate high levels of iodine. The macroalgae contributed significantly to the dietary practices of Inuit populations (Andersen et al., 2019). Another study in the Arabian Gulf provided baseline data on iodine and fluorine levels from 11 common seaweed species (Al-Adila et al., 2020). However, all these studies were restricted to algal macrophytes. Moreover, no investigation on algal halogen levels has been conducted in the Bay of Bengal region of Bangladesh.

Despite the ecological and physiological significance of algal macrophytes, previous studies were primarily metal accumulation-centric, while the important negative anions remain underexplored, particularly in the context of the northern Bay of Bengal. The only coral-bearing island in Bangladesh, St. Martin's Island, is a vital marine ecosystem that supports diverse macroalgal and microalgal species (Rahman et al., 2026). Extensive research has documented a wide range of algal diversity on this island. Approximately 45 taxa of green algae, including notable species *Caulerpa* sp. and *Cladophora* sp., and additionally, 56 brown algal taxa, including *Sargassum* sp., *Turbinaria* sp., and *Spatoglossum* sp., were recorded. Moreover, 95 red algal taxa were dominated by *Gracilaria* sp., *Hypnea* sp., and *Ceramium* sp. (Aziz & Rahman, 2011). These algae form the base of the food web and are crucial for nutrient cycling, habitat structuring, and raw material for commercial bioresources. However, studies investigating the chemical composition of these algae, particularly in terms of negative ions, remained unaddressed. This study aimed to quantify cellular chlorine, fluorine, nitrate, and sulfate in both macroalgae and microalgae from St. Martin's Island. This novel baseline data on anion concentrations in marine algae from this region will contribute to a better understanding of algal biochemical composition and its implications for marine ecosystem health and environmental monitoring.

2. Materials and methods

2.1. Study location

The investigation zone lies along the coast of St. Martin's Island, Bangladesh (Figure 1). This region is enriched with diverse marine algal flora and vibrant coral ecosystems, having high ecological significance. The coral reef containing St. Martin's Island is located on the southernmost end of Bangladesh (between 20° 34′–20° 39′ N and 92° 18′–92° 21′ E). It features a sandy, rocky bottom and weak wave action (Islam et al., 2021). Mean water temperature and salinity have been reported as 27.53°C and 32.76 ppt, respectively, in this area (Kashem et al., 2019). These environmental conditions are favorable for both macro- and microalgal vegetation growth. Additionally, St. Martin's Island contributes as a house of carbon sequestration via a number of marine plant and animal habitats supporting biodiversity and regulating nutrient cycling, the impact of which extends to the Bay of Bengal. Moreover, this area infuses US$33.6 million into the local economy each year (Sultana et al., 2018). The environmental and economic attributes make this sole coral island of Bangladesh a crucial area for investigation.

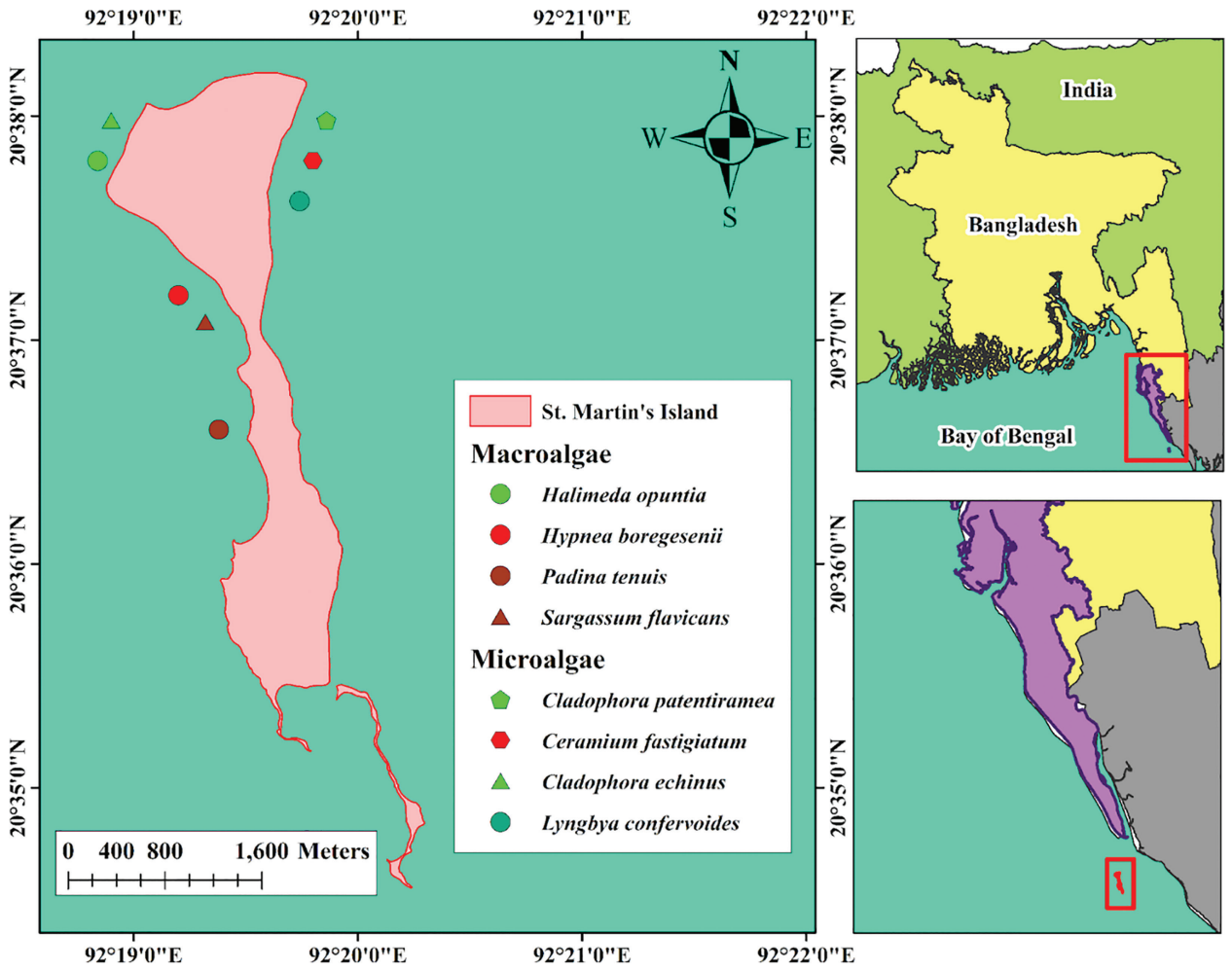

Figure 1

Microalgae and macroalgae collection site on St. Martin's Island of Bangladesh.

2.2. Sample collection, identification and preparation

Sampling stations were chosen to encompass all the available algae along the coast of St. Martin's Island during post-monsoon (November). Algal specimens were collected following Al-Adila et al. (2020) during the ebb tide phase from supratidal to subtidal zones. To minimize contamination, nitrile gloves and pre-cleaned stainless plastic tools were used. Each sample was collected into a separate sterile plastic bag. Free-floating specimens were carefully separated from debris, while attached algae were handpicked from rocks composed of argillaceous limestone, calcareous sandstone, fossiliferous conglomerates, and coralline limestone. On-site, samples were gently rinsed with filtered seawater to remove sand, epiphytes, and other debris. Subsequently, the fresh samples were frozen, providing external ice cube support, brought to the lab, and then given three further washes through deionized water. Samples were immediately frozen at –20°C to prevent chemical changes before analysis.

This study represents an initial baseline report of a halogen-focused assessment of algae from St. Martin's Island, Bangladesh. Algal communities on the island occur in narrow, patchy belts restricted by tidal exposure and reef topography. The sampling design targeted ecological coverage of locally available species during a single well-defined period rather than seasonal or spatial replication due to the short post-monsoon collection window and limited accessibility during ebb tide. This approach provides an initial baseline inventory but does not capture temporal variability or within-species spatial variation, which are acknowledged as limitations of the present dataset.

The identification and taxonomic description of the collected seaweed species were done by consulting standard literature (Borowitzka, 2002; Islam, 1976; Prud'homme van Reine & Torno, 2002; Starmach et al., 1966). Morphological features, including thallus structure, reproductive organs, and filament arrangement, were examined; microscopes were used for microalgal species, and a magnifying glass was used for macroalgae. Representative images were taken to document morphology. Biomass of eight algal species (Supplementary Fig. 1), namely, *L. confervoides* Ag., *C. echinus* (Bias.) Kg., *C. patentiramea* (Mont.) Kg., *Halimeda opuntia* (L.) Lamx., *Padina tenuis* (*C. Agardh*) Bory, *Sargassum flavicans* J. Ag., *Ceramium fastigeatum* Harvey, and *H. boergesenii* Tak. Tanaka, were carefully separated and air-dried at ambient temperature (~25°C) after thawing to preserve halogen content. The dried biomass of each individual species was ground separately into a fine powder using a mortar and pestle, which was thoroughly cleaned between species to avoid cross-contamination. Approximately 1 g of the ground powdered sample was measured through analytical balance (precision ±0.1 mg) and was transferred to a 15 mL centrifuge tube; to it 10 mL of deionized water was added. The mixture was vortexed at medium speed (~2000 rpm) for 5 min vigorously to ensure thorough mixing. For the next 30 min, samples were sonicated in an ultrasonic bath (40 kHz, 25°C) to facilitate ion release into the aqueous phase. Eventually, the samples were centrifuged (5000 rpm) for 10 min at 4°C. It helped in the separation of solid residue. The algal water extract (supernatant) was collected and filtered through a pre-rinsed 0.45 µm PVDF syringe filter (Millex-HV; MilliporeSigma, Burlington, MA, USA), with separate filters for each sample to prevent cross-contamination.

2.3. Reagents

All reagents were of ion chromatography (IC) grade. The mobile phase salts, sodium carbonate (Na_2CO_3) and sodium bicarbonate ($NaHCO_3$), ensured a minimal ionic background. Ultrapure water (18.2 MΩ•cm) was used for all preparations. All standards, working solutions, and eluents were freshly prepared and filtered through 0.45 µm PVDF membranes (Millex HV) before use.

2.4 Halogen and oxyanion level determination

Anion concentrations (F^-, Cl^-, NO_3^-, SO_4^{2-}) in algal extracts were quantified using IC on a Thermo Scientific Dionex ICS-1100 system (Thermo Fisher Scientific Inc., Massachusetts, U.S.A.) equipped with a quaternary pump, an autosampler (25 µL loop), a 30°C thermostatted column compartment, and suppressed conductivity detection. Separation was achieved using a Dionex IonPac™ AS22 analytical column (4 × 250 mm) and an AG22 guard column (4 × 50 mm), following the manufacturer-recommended operating conditions (TFS, 2014).

Extracts were diluted 1:10 in ultrapure water to reduce matrix load and ensure that analyte levels remained within the calibration range. The diluted extracts were clear and particle-free and were injected at a volume of 10 µL using the 25 µL loop. The system was equilibrated for 20 min with the carbonate eluent before the first run, and the conductivity detector operated within a range of 0–50 µS.

The eluent consisted of 4.5 mM Na_2CO_3 and 1.4 mM $NaHCO_3$, filtered through a 0.22 µm membrane and degassed by vacuum aspiration. Fresh eluent was prepared every 48 hr and delivered at a flow rate of 1.2 mL · min^{-1}. Suppression was performed using an ASRS™ 300 suppressor (Thermo Fisher Scientific, Waltham, MA, USA) operated at 50 mA in external water mode, with suppressor water supplied at 5 mL · min^{-1} (Jackson, 2000).

The total runtime per analysis was 15 min, with typical retention times of 2.5 min (F^-), 4.5 min (Cl^-), 6.5 min (NO_3^-), and 8.0 min (SO_4^{2-}). A 5-min re-equilibration step between injections was used to maintain retention-time consistency and baseline stability.

IC was selected because it provides reliable separation and quantification of water-soluble inorganic anions at low concentrations and small injection volumes, which fits the limited algal biomass available in this study (Jackson, 2000). The extraction with deionized water was used to target the physiologically accessible fraction rather than the total halogen content (Gómez-Ordóñez et al., 2010). This approach allowed consistent recovery of chloride, fluoride, nitrate, and sulfate without the need for complex digestion steps, making the method appropriate for the exploratory nature of the analysis.

2.5. Analytical quality control, calibration, and performance

A certified multi-anion stock solution (Thermo Scientific Dionex Seven Anion Standard II, 1000 mg · L^{-1} each anion) was used to prepare working standards. Calibration standards were prepared in ultrapure water at 0.1, 0.25, 0.5, 1.0, 2.5, and 5.0 mg · L^{-1} for F^-, Cl^-, NO_3^-, and SO_4^{2-} using Class A volumetric flasks and calibrated micropipettes. External calibration curves were generated by plotting peak area against

concentration, showing linearity across the full range ($R^2 \geq 0.999$).

Calibration verification used an independent 2.0 mg · L^{-1} checkpoint standard injected at the start and end of each batch. A deviation greater than ±5% triggered rejection and reanalysis of the batch. Sample quantification was performed using Chromeleon software (version 6.8) with automatic integration, baseline correction, and retention-time confirmation within ±0.1 min of standards.

Quality-control measures included the injection of an instrument blank and the 2.0 mg · L^{-1} standard after every 10 samples to monitor detector drift and contamination. Runs were repeated if blank signals exceeded baseline +3 × SD (standard deviation) or if the QC (quality control) standard deviated by more than ±5%. The chromatographic conditions used during calibration matched those established during method validation to ensure consistency.

2.6. Method validation

Method validation was carried out to ensure that the ion chromatographic measurements remained accurate, precise, and free from contamination throughout the experiment. Procedural blanks prepared with fresh eluent were analyzed at the start of each batch and after every 10 injections to track baseline stability and any sign of carryover. Blank values were documented for every run, and corrections were applied when the blank exceeded normal baseline fluctuations. If a blank showed an unexpected rise in any target anion, the system was flushed, the eluent was replaced, and both the blank and the affected samples were reanalyzed to avoid false positives.

All sample handling was done with acid-washed Class A glassware, calibrated micropipettes, and clean work surfaces to minimize chloride or nitrate intrusion from the laboratory environment. Fresh gloves were used during standard and sample preparation, and all containers were rinsed with ultrapure water immediately before use. These steps kept extraneous anions low enough that blank signals stayed within the expected noise range.

Accuracy and matrix effects were evaluated using laboratory-fortified blanks and laboratory-fortified matrix samples prepared at 0.5, 1.0, and 2.5 mg · L^{-1}. Each level was analyzed in triplicate, and recoveries between 80% and 120% were considered acceptable. Precision was assessed through repeated injections of a 2.0 mg · L^{-1} quality-control standard, which also served as the calibration-verification point. Results were required to remain within ±5% of the expected concentration. Any deviation beyond this range triggered reinjection and, if needed, full recalibration.

External calibration standards were prepared from the certified multi-anion stock solution at 0.1–5.0 mg · L^{-1} using Class A volumetric flasks and calibrated micropipettes. Peak areas were plotted against concentration, producing linear calibration curves across the full range ($R^2 \geq 0.999$). Analyte identity was confirmed through retention-time agreement within ±0.1 min of the standards. Method detection limits were determined following EPA Method 300.1 using seven replicate injections of a 0.1 mg · L^{-1} standard. The resulting MDLs (Method Detection Limits) were approximately 0.01 mg · L^{-1} for F^-, 0.02 mg · L^{-1} for Cl^- and NO_3^-, and 0.05 mg · L^{-1} for SO_4^{2-}. All chromatographic conditions used during validation matched the conditions maintained throughout routine analysis to ensure consistent performance of the AS22 column and the carbonate eluent system (Jackson, 2000).

2.7. Data treatment

The analysis focused on the water-extractable inorganic anion fraction. This reflects the readily available ionic pool in algal tissues and aligns to produce a descriptive profile rather than a total halogen inventory. Anion concentrations were normalized to algal fresh weight (mg · mL^{-1} FW). Due to methodological constraints, this approach quantifies only water-soluble inorganic anions and does not account for organically bound halogen species.

2.8. Statistical treatment of data

The analysis was designed to be exploratory and descriptive rather than inferential. Each species was represented by a single prepared extract, and the anion concentrations reflect point measurements obtained from individual IC runs. Uncertainty was managed through instrument quality control, blank correction, and calibration procedures instead of analytical replication. Comparisons among species are therefore interpreted in a qualitative sense, focusing on relative patterns rather than statistical testing.

3. Results and discussions

This dataset (Table 1) represents the first set of anion measurements for these algal species from Saint Martin's Island, Bangladesh. Therefore, numerical comparison with existing studies is inherently limited. Most published work either focuses on different

Table 1

Halogen and oxyanion profile of marine algae (mg · g^{-1} of dry algal biomass) from St. Martin's Island of Bangladesh.

Algae type	Group	Species	Cl^- (mg · g^{-1})	F^- (mg · g^{-1})	SO_4^{2-} (mg · g^{-1})	NO_3^- (mg · g^{-1})
Macroalgae	Brown algae	*P. tenuis*	10.22	-	21.35	-
		S. flavicans	7.22	0.04	6.33	0.24
	Green algae	*H. opuntia*	4.25	-	2.88	0.32
	Red algae	*H. boergesenii*	3.83	0.22	3.01	0.22
Microalgae	Green algae	*C. echinus*	4.1	-	2.88	0.32
		C. patentiramea	11.18	-	11.79	-
	Cyanophyta	*L. confervoides*	5.86	0.1	3.93	0.06
	Red algae	*C. fastigiatum*	23.94	-	7.98	0.24

species, or the taxonomy does not match even at the genus level, and the available data rarely report the same suite of anions. Therefore, instead of numerical anchor comparisons, the interpretation relies on broader trends and patterns of halogen uptake in the local algal species combined with the influence of local biogeochemistry.

This pattern reflects the natural chemistry of seawater around Saint Martin Island, where chloride is overwhelmingly dominant, and fluoride occurs only in trace amounts. Sulfate is also naturally abundant in marine water, whereas nitrate remains relatively limited in oligotrophic reef settings (Pilson, 2012). The distribution of the ions in the algae (Supplementary Figs. 2-9), therefore, aligns with what is expected in a coral-associated, oligotrophic setting.

The two brown algae showed contrasting patterns. *P. tenuis* contained 10.22 mg · g^{-1} of chloride and 21.35 mg · g^{-1} of sulfate, which appeared elevated compared with the other species in this dataset. Notably. The elevated sulfate likely reflects its need for sulfated polysaccharides that support photoprotection and oxidative stress management, a trait often seen in *Padina* sp. in high-light, shallow reef habitats (Wang et al., 2023). Fluoride and nitrate were below the level of detection in the algae. The absence of fluoride and nitrate is either the consequence of restricted environmental availability or a selective accumulation mechanism. *S. flavicans*, in contrast, accumulated all four ions (7.22 mg · g^{-1} of chloride, 0.04 mg · g^{-1} of fluoride, 6.33 mg · g^{-1} of sulfate, and 0.24 mg · g^{-1} of nitrate), suggesting a broad physiological capacity to use whatever anions are available in the surrounding water.

H. opuntia, a calcifying green macro-algae, contained chloride (4.25 mg · g^{-1}), sulfate (2.88 mg · g^{-1}), and nitrate (0.32 mg · g^{-1}) but no fluoride. This species forms a calcium carbonate structure, and in the local reef setting, its calcium carbonate matrix can bind fluoride into insoluble CaF_2, reducing free fluoride in the tissue, which might explain the absence of detectable F^- by forming insoluble CaF_2 (Castro-Sanguino et al., 2020).

From the red algal group, *Hy. boergesenii* contained all the anions. It demonstrated 3.83 mg · g^{-1} of chloride, 0.22 mg · g^{-1} of fluoride, 3.01 mg · g^{-1} of sulfate, and 0.22 mg · g^{-1} of nitrate. Notably, fluoride appeared more concentrated in this species than in the rest. In the context of Saint Martin Island, this suggests that this species is able to retain a slightly greater share of the available fluoride.

Two species from the microalgal Chlorophyta were analyzed. *C. echinus* contained 4.10 mg · g^{-1} of chloride, 2.88 mg · g^{-1} of sulfate, and 0.32 mg · g^{-1} of nitrate; however, fluoride was below the limit of detection. Additionally, *C. patentiramea* from the same genus displayed the highest chloride concentration among the green algae at 11.18 mg · g^{-1}, along with 11.79 mg · g^{-1} of sulfate; however, fluoride and nitrate were not detected. The shared absence of fluoride in both species reflects low fluoride bioavailability around Saint Martin Island. Green microalgae are also known to rely on membrane structures that limit the passive movement of certain anions, which may further reduce fluoride retention (Pitre et al., 2014). In this dataset, the pattern most likely reflects the combination of environmental scarcity and the characteristic ion-handling properties of these Chlorophyta species.

L. confervoides from the Cyanophyta group had 5.86 mg · g^{-1} of chloride, 0.10 mg · g^{-1} of fluoride, 3.93 mg · g^{-1} of sulfate, and 0.06 mg · g^{-1} of nitrate. Notably, Cyanophyta are sensitive to fluorides (Kanad et al., 2000) and are the only species found to accumulate fluoride amongst microalgae in this study. Moreover, the nitrogen fixation characteristics of Lyngbya can reduce the nitrate dependency, resulting

in lower nitrate ion accumulation in typical coastal conditions. (Zehr, 2011).

C. fastigiatum from red microalgae stood out with a notably higher chloride (23.94 mg · g^{-1}) level relative to the others, along with 7.98 mg · g^{-1} of sulfate and 0.24 mg · g^{-1} of nitrate. Fluoride was not detected in the species. This strong chloride accumulation is consistent with the species' need to regulate its internal osmotic balance in a coastal area like southeastern Bangladesh, where salinity fluctuates with tidal mixing and seasonal freshwater discharge. (van Ginneken, 2018).

The consistent presence of chloride and sulfate in every macroalgal and microalgal species reflects their steady availability in the waters around St. Martin's Island. In contrast, the irregular accumulation of fluoride and nitrate mirrors their limited presence in this small coral-bearing island system, as well as species-specific uptake strategies. These differences shape how each alga grows and competes under local conditions, and together they contribute to the broader community structure found along the reef flats and lagoonal margins of St. Martin's.

Elevated chloride in coastal waters can disrupt fish egg swelling and early development (Lawson & Jackson, 2024), which is particularly relevant for St. Martin's Island, where many reef-associated juveniles rely on stable nearshore conditions. The chloride absorbed by both macroalgae and microalgae in this study offers an early signal of such shifts because these species tend to respond quickly to changes in the island's shallow, tide-influenced waters. Sulfate levels in the algae also reflect local sulfate reduction potential, a key step in biogeochemical cycling that shapes the mobility and toxicity of heavy metals in this coral-bearing environment; the organic matter produced by algae can support sulfate-reducing bacteria in driving this process (Ayala-Parra et al., 2016). Fluoride was detected in only a few species, which points to its limited availability around the island. Measuring fluoride in algal tissue can help identify pockets of contamination and provide an early warning of chemical disturbances since algal communities react rapidly to changes in water chemistry (Sen et al., 2013). Nitrate remained low across all samples, yet its presence still matters because elevated nitrate around the island has the potential to fuel nuisance algal blooms that can affect local biota if not monitored and managed (Wang et al., 2020). Taken together, these anion patterns illustrate how algae integrate local environmental signals and can serve as useful indicators for understanding and safeguarding the ecosystem health of St. Martin's Island.

It is important to consider the nature of the sample preparation and analytical design. The use of deionized water targeted only the readily soluble ionic fraction, while iodine and bromine often occur in organically bound forms that aqueous extraction does not efficiently release (Al-Adilah et al., 2022; Küpper et al., 2013). These undissolved fractions were outside the scope of the current work and therefore not detected. Each species was represented by a single extract and a single IC run, consistent with the exploratory framework of this study. The values reflect point measurements of the water-extractable fraction under controlled conditions. Even without inferential statistics, the patterns observed across chloride, sulfate, fluoride, and nitrate provide a first description of the physiologically accessible ionic forms present in the algal biomass.

4. Conclusions

This study offers the first baseline view of cellular halogens and oxyanions in the macro- and microalgae of St. Martin's Island, an area of ecological and economic value in the North Bay of Bengal. Chloride and sulfate appeared consistently across all species, which aligns with their central roles in algal physiology and the chemistry of the island's waters. In contrast, the limited presence of fluoride and nitrate reflects both their restricted availability in this coral-associated setting and the species-specific uptake patterns observed in the local flora. These results add the first regional dataset on algal halogen and oxyanion composition from this island with simultaneous limitations and boundaries. The sampling design was tailored to document a first inventory using the species available during the post-monsoon period, when algal abundance is highest. Consequently, the research does not capture seasonal shifts or finer spatial variability within species. It reflects the exploratory nature of the dataset rather than a gap in analytical rigor. Even within this scope, the findings provide a useful foundation for environmental assessment and for understanding how local algae interact with the ion-rich waters around the island. Future studies can build on this by incorporating seasonal sampling, broader spatial coverage, and extraction methods that resolve both inorganic and organically bound halogens, including iodine and bromine, to complete the halogen profile and offer a more comprehensive biochemical picture of the region's algal communities.

Acknowledgment

We thank Saiful Alam Shakil and the local people of St. Martin Island for cooperating and helping us collect the algae.

Author contributions

Swachsa Rahman: Conceptualization, sampling, analysis, and writing the original draft; Arnob Ghosh: Data analysis, visualization, writing; Md. Biplob Hasan: Sampling and Formal Analysis; Moniruzzaman Khondker: Identification of marine algal species, writing in part, and editing of the manuscript; Fateeha Noor: Reviewing the manuscript. Mir Shariful Islam: visualization, Reviewing the manuscript; Mustafizur Rahman Naim: Analysis, Reviewing the manuscript; Mahmudul Hasan: Supervision, visualization, Reviewing the manuscript.

Funding

This study was supported by the National Science and Technology Fellowship from the Ministry of Science and Technology, Government of Bangladesh, awarded for master's thesis research in 2023.

Availability of data and materials

The data that support the findings of this study are available from the corresponding author at the corresponding email address upon reasonable request.

Statements and declarations

Conflict of interest

The authors have no conflicts of interest to declare.

Ethical declaration

Not applicable.

Consent to participate

Not applicable.

Consent for publication

All the authors have given their consent for publication.

References

Al-Adilah, H., Feiters, M. C., Carpenter, L. J., Kumari, P., Carrano, C. J., Al-Bader, D., & Küpper, F. C. (2022). Halogens in seaweeds: Biological and environmental significance. *Phycology, 2*(1), 132–171. https://doi.org/10.3390/phycology2010009

Al-Adila, H., Peters, A., Al-Bader, D., Raab, A., Akhdhar, A., Feldmann, J., & Küpper, F. (2020). Iodine and fluorine concentrations in seaweeds of the Arabian Gulf identified by morphology and DNA barcodes. *Botanica Marina, 63(6)*, 509–519. https://doi.org/10.1515/bot-2020-0049

Andersen, S., Noahsen, P., Rex, K. F., Florian-Sørensen, H. C., & Mulvad, G. (2019). Iodine in edible seaweed, its absorption, dietary use, and relation to iodine nutrition in arctic people. *Journal of Medicinal Food, 22*(4), 421–426. https://doi.org/10.1089/jmf.2018.0187

Ayala-Parra, P., Sierra-Alvarez, R., & Field, J. A. (2016). Algae as an electron donor promoting sulfate reduction for the bioremediation of acid rock drainage. *Journal of Hazardous Materials, 317*, 335–343. https://doi.org/10.1016/j.jhazmat.2016.06.011

Aziz, A., & Rahman, M. T. (2011). Marine algae of St. Martin's Island, Bangladesh. XII. New records of red and green algae. *Bangladesh Journal of Botany, 40*(1), 41–45. https://doi.org/10.3329/bjb.v40i1.7996

Borowitzka, M. A. (2002). Plant resources of South-East Asia, No. 15 (1). Cryptogams: Algae. *Botanica Marina, 45*(6),593–594. https://doi.org/10.1515/BOT.2002.064

Castro-Sanguino, C., Bozec, Y., & Mumby, P. (2020). Dynamics of carbonate sediment production by Halimeda: Implications for reef carbonate budgets. *Marine Ecology Progress Series, 639*, 91–106. https://doi.org/10.3354/meps13265

Chen, Y., Lan, L., Zhang, J., Wang, Q., Liu, Y., Li, H., Gong, Q., & Gao, X. (2023). Physiological impacts of nitrogen starvation and subsequent recovery on the red seaweed *Grateloupia turuturu* (Halymeniaceae, Rhodophyta). *Sustainability, 15*(9), 7032. https://doi.org/10.3390/su15097032

Giordano, M., Norici, A., Ratti, S., & Raven, J. A. (2008). Role of Sulfur for Algae: Acquisition, Metabolism, Ecology and Evolution. In: Hell, R., Dahl, C., Knaff, D., Leustek, T. (eds) Sulfur Metabolism in Phototrophic Organisms. Advances in Photosynthesis and Respiration, vol. 27. Springer, Dordrecht. https://doi.org/10.1007/978-1-4020-6863-8_20

Gómez-Ordóñez, E., Alonso, E., & Rupérez, P. (2010). A simple ion chromatography method for inorganic anion analysis in edible seaweeds. *Talanta, 82*(4), 1313–1317. https://doi.org/10.1016/j.talanta.2010.06.062

Islam, A. K. M. N. (1976). In J. Cramer (Ed.), *Contribution to the study of the marine algae of Bangladesh*. https://books.google.com.bd/books?id=iaQLAQAAIAAJ

Islam, M. M., Hasan, J., Ali, M. Z., & Hoq, M. E. (2021). Culture of three seaweed species in Cox's Bazar Coast, Bangladesh. *Bangladesh Journal of Zoology, 49*(1), 47–56. https://doi.org/10.3329/bjz.v49i1.53681

Jackson, P. E. (2000). Ion chromatography in environmental analysis. In R. A. Meyers (Ed.), *Encyclopedia of analytical chemistry: Applications, theory, and instrumentation* (pp. 2779–2801). John Wiley & Sons https://doi.org/10.1002/9780470027318.a0835

Joye, S. B., Bowles, M. W., & Ziervogel, K. (2022). Marine Biogeochemical Cycles. In: Stal, L.J., Cretoiu, M.S. (eds) The Marine Microbiome. The Microbiomes of Humans, Animals, Plants, and the Environment, vol. 3. Springer, Cham. https://doi.org/10.1007/978-3-030-90383-1_15

Kashem, M., Nahian, S., & Kibria, M. (2019). Assessment of physico-chemical status of coastal seawater of the Saint Martin's Island, Bangladesh. *International Journal of Scientific and Engineering Research, 10(3)*, 84–91.

Küpper, F. C., Carpenter, L. J., Leblanc, C., Toyama, C., Uchida, Y., Maskrey, B. H., Robinson, J., Verhaeghe, E. F., Malin, G., Luther, G. W., Kroneck, P. M. H., Kloareg, B., Meyer-Klaucke, W., Muramatsu, Y., Megson, I. L., Potin, P., & Feiters, M. C. (2013). In vivo speciation studies and antioxidant properties of bromine in *Laminaria digitata* reinforce the significance of iodine accumulation for kelps. *Journal of Experimental Botany, 64*(10), 2653–2664. https://doi.org/10.1093/jxb/ert110

Lan, J., Liu, P., Hu, X., & Zhu, S. (2024). Harmful algal blooms in eutrophic marine environments: Causes, monitoring, and treatment. *Water, 16*(17), 2525. https://doi.org/10.3390/w16172525

Lawson, L., & Jackson, D. A. (2024). Water quality patterns in at-risk fish habitat: Assessing frequency and cumulative duration of chloride guideline exceedance during early life stages of an endangered fish. *Ecological Indicators, 168,* 112707. https://doi.org/10.1016/j.ecolind.2024.112707

Pilson, M. E. Q. (2012). *An introduction to the chemistry of the sea*. Cambridge University Press. https://doi.org/10.1017/CBO9781139047203

Pitre, D., Boullemant, A., & Fortin, C. (2014). Uptake and sorption of aluminium and fluoride by four green algal species. *Chemistry Central Journal, 8*(1), 8. https://doi.org/10.1186/1752-153X-8-8

Prud'homme van Reine, Prud'homme van Reine, W. F., & Trono Jr, G. C. (Eds.). (2001). *Plant resources of South-East Asia: No. 15(1). Cryptogams: Algae*. Backhuys Publishers.

Rahman, Swachsa, Md Zia Uddin Al Mamun, Fateeha Noor, Mir Shariful Islam, Moniruzzaman Khondker, Mahmudul Hasan, Md Tazinur Rahman, and Mustafizur Rahman Naim. (2025). Marine algae from coastal Bangladesh: Insights into nutritional potential and dietary implications. *Regional Studies in Marine Science* 93, 104650.

Romarís-Hortas, V., Bermejo-Barrera, P., Moreda-Piñeiro, J., & Moreda-Piñeiro, A. (2012). Speciation of the bio-available iodine and bromine forms in edible seaweed by high performance liquid chromatography hyphenated with inductively coupled plasma-mass spectrometry. *Analytica Chimica Acta, 745*, 24–32. https://doi.org/10.1016/j.aca.2012.07.035

Rondan, F., Mendes Pereira, R., Aline da Silva, A., Tessmer Scaglioni, P., Colepicolo, P., & Foster Mesko, M. (2024a). New strategy for single analysis of Antarctic seaweed for halogen and sulfur determination. *Microchemical Journal, 199(6)*, 110027. https://doi.org/10.1016/j.microc.2024.110027

Rondan, F. S., Pisarek, P., Godin, S., Szpunar, J., & Mesko, M. F. (2024b). Characterization of halogen species in seaweeds from the Antarctic using a multi-technique approach. *Journal of Trace Elements in Medicine and Biology, 83(8)*, 127396. https://doi.org/10.1016/j.jtemb.2024.127396

Sen, B., Tahir, M., Sonmez, F., Turan Kocer, M. A., & Canpolat, O. (2013). Relationship of algae to water pollution and waste water treatment. In W. Elshorbagy & R. K. Chowdhury (Eds.), *Water Treatment* (pp. 335–354). InTech Open. https://doi.org/10.5772/51927

Starmach, K., Nauk, I. B., & Polska, A. (1966). *Flora słodkowodna Polski: Starmach, K. Cyanophyta-sinice. Glaucophyta glaukofity*. Państwowe Wydawn. https://books.google.com.bd/books?id=DRkIAQAAMAAJ

Sultana, I., Alam, S. M. I., & Das, D. K. (2018). An annotated avifaunal checklist of the Saint Martin's Island of Bangladesh. *Journal of the Asiatic Society of Bangladesh, Science, 44*(2), 149–158. https://doi.org/10.3329/jasbs.v44i2.46557

Trégarot, E., D'Olivo, J. P., Botelho, A. Z., Cabrito, A., Cardoso, G. O., Casal, G., Cornet, C. C., Cragg, S. M., Degia, A. K., Fredriksen, S., Furlan, E., Heiss, G., Kersting, D. K., Maréchal, J. P., Meesters, E., O'Leary, B. C., Pérez, G., Seijo-Núñez, C., Simide, R., van der Geest M., de Juan, S. (2024). Effects of climate change on marine coastal ecosystems – A review to guide research and management. *Biological Conservation, 289*, 110394. https://doi.org/10.1016/j.biocon.2023.110394

Thermo Scientific,TSF(2014). *Product manual for Dionex IonPac AS22 and AS22-Fast columns* (Revision 08). https://documents.thermofisher.com/TFS-Assets/CMD/manuals/Man-065119-IC-IonPac-AS22-Fast-Man065119-EN.pdf

van Ginneken, V. (2018). Some mechanism seaweeds employ to cope with salinity stress in the harsh euhaline oceanic environment. *American Journal of Plant Sciences, 09*(06), 1191–1211. https://doi.org/10.4236/ajps.2018.96089

Wang, H., Wang, G., & Gu, W. (2020). Macroalgal blooms caused by marine nutrient changes resulting from human activities. *Journal of Applied Ecology, 57*(4), 766–776. https://doi.org/10.1111/1365-2664.13587

Wang, L., Jayawardena, T. U., Kim, Y. S., Wang, K., Fu, X., Ahn, G., Cha, S. H., Kim, J. G., Lee, J. S., & Jeon, Y. J. (2023). Anti-melanogenesis and anti-photoaging effects of the sulfated polysaccharides isolated from the brown seaweed *Padina boryana*. *Polymers, 15*(16), 3382. https://doi.org/10.3390/polym15163382

Woodroffe, C. D., Evelpidou, N., Delgado-Fernandez, I., Green, D. R., Karkani, A., & Ciavola, P. (2023). Coastal Systems: The Dynamic Interface Between Land and Sea. In: Bański, J., Meadows, M. (eds) Research Directions, Challenges and Achievements of Modern Geography. Advances in Geographical and Environmental Sciences. Springer, Singapore. https://doi.org/10.1007/978-981-99-6604-2_11

Zehr, J. P. (2011). Nitrogen fixation by marine cyanobacteria. *Trends in Microbiology, 19*(4), 162–173. https://doi.org/10.1016/j.tim.2010.12.004

Supplementary Material

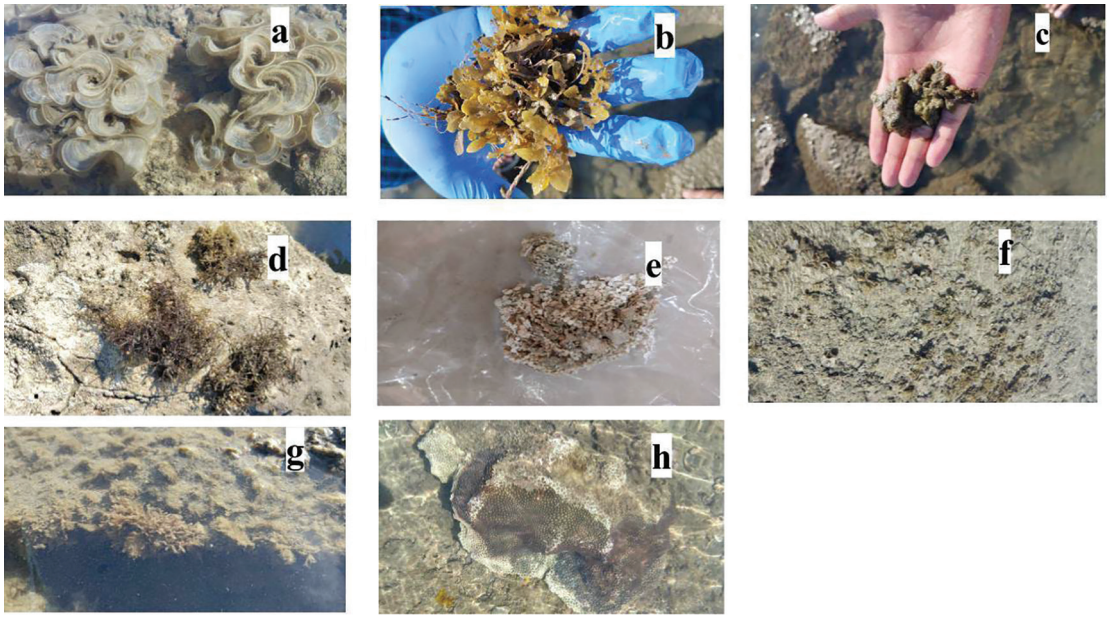

Figure S1

Algal species collected in this study: **(A)** *P. tenuis* (*C. Agardh*) Bory **(B)** *S. flavicans* J. Ag. **(C)** *H. opuntia* (L.) Lamx. **(D)** *H. boergesenii* Tak. Tanaka **(E)** *C. echinus* (Bias.) Kg. **(F)** *C. patentiramea* (Mont.) Kg. **(G)** *L. confervoides* Ag. **(H)** *C. fastigeatum* Harvey.

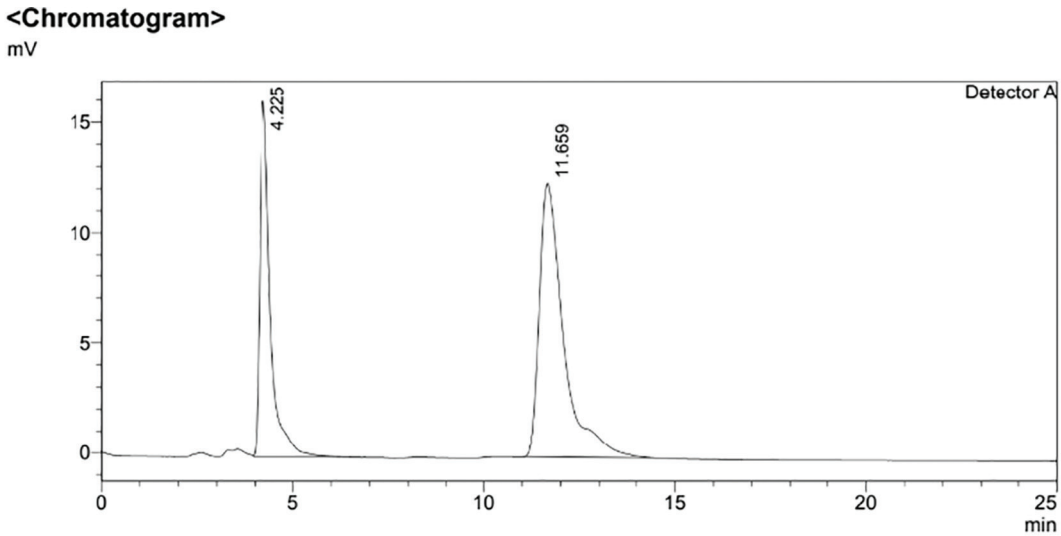

<Peak Table>

Detector A

Peak#	Ret. Time	Area	Height	Conc.	Unit	Mark	Name
1	4.225	325160	16138	51.088	mg/L	V	CL
2	11.659	544268	12424	106.758	mg/L		SO4
Total		869428	28562				

Figure S2

IC-chromatogram of *P. tennuis*. IC, ion chromatography.

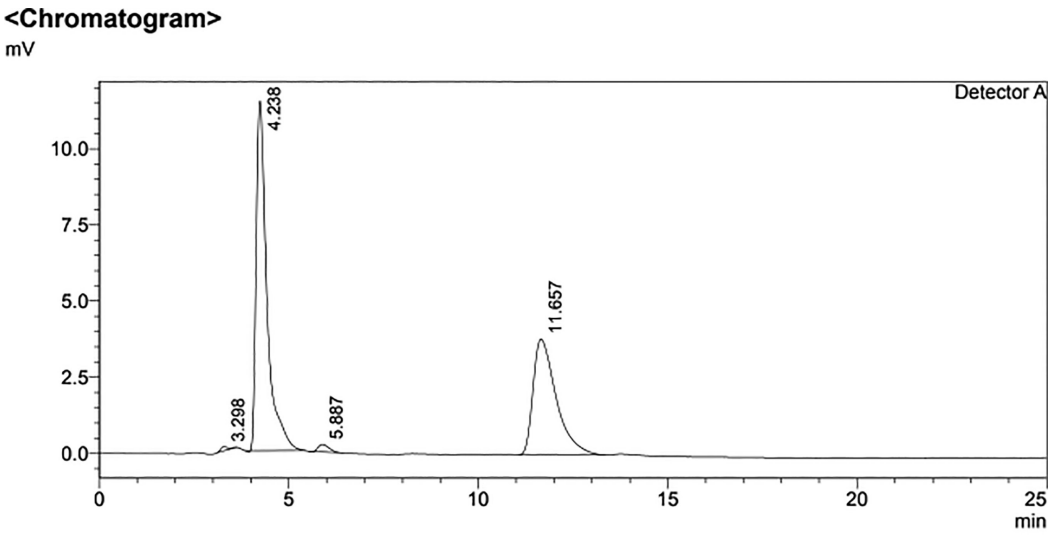

<Peak Table>
Detector A

Peak#	Ret. Time	Area	Height	Conc.	Unit	Mark	Name
1	3.298	1968	135	0.197	mg/L	M	F
2	4.238	229717	11481	36.093	mg/L	M	CL
3	5.887	4943	248	1.223	mg/L	M	NO3
4	11.657	161322	3803	31.643	mg/L		SO4
Total		397950	15667				

Figure S3

IC-chromatogram of *S. flavicans*. IC, ion chromatography.

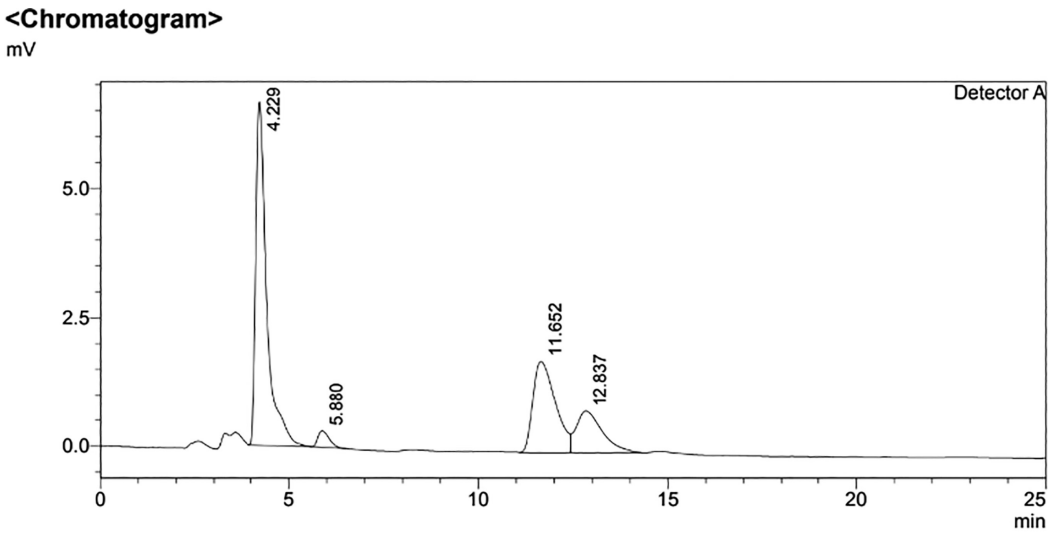

<Peak Table>
Detector A

Peak#	Ret. Time	Area	Height	Conc.	Unit	Mark	Name
1	4.229	135264	6658	21.252	mg/L	M	CL
2	5.880	6486	316	1.604	mg/L	M	NO3
3	11.652	73426	1787	14.403	mg/L		SO4
4	12.837	38426	804	0.000		V	
Total		253603	9565				

Figure S4

IC chromatogram of *H. opuntia*. IC, ion chromatography.

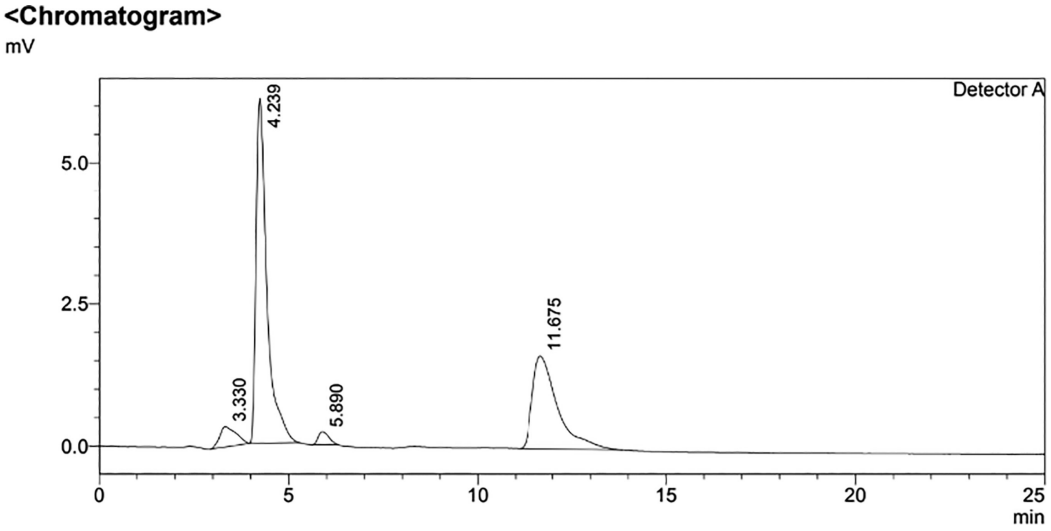

<Peak Table>
Detector A

Peak#	Ret. Time	Area	Height	Conc.	Unit	Mark	Name
1	3.330	10833	360	1.082	mg/L		F
2	4.239	121951	6079	19.161	mg/L	M	CL
3	5.890	4463	227	1.104	mg/L	M	NO3
4	11.675	76775	1633	15.060	mg/L		SO4
Total		214023	8298				

Figure S5

IC chromatogram of *H. boergesenii*. IC, ion chromatography.

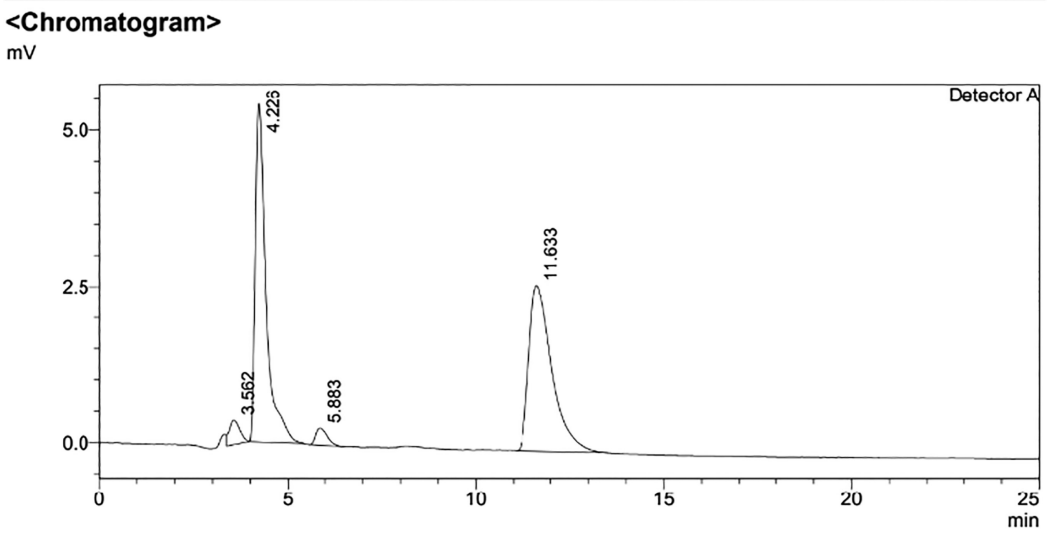

<Peak Table>
Detector A

Peak#	Ret. Time	Area	Height	Conc.	Unit	Mark	Name
1	3.562	7616	393	0.000		V	
2	4.226	108270	5413	17.011	mg/L	M	CL
3	5.883	5777	274	1.429	mg/L	M	NO3
4	11.633	113480	2661	22.259	mg/L		SO4
Total		235143	8740				

Figure S6

IC chromatogram of *C. echinus*. IC, ion chromatography.

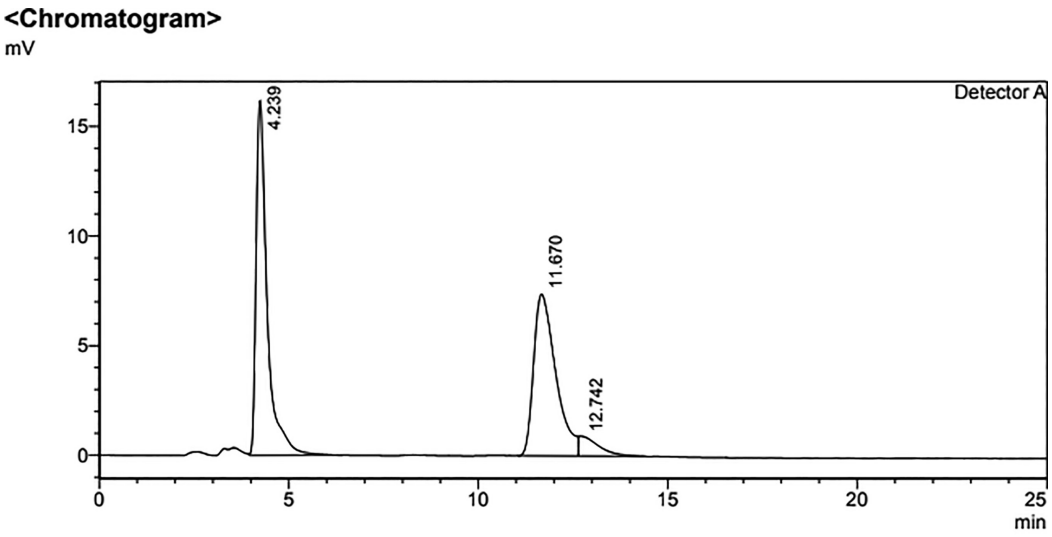

<Peak Table>
Detector A

Peak#	Ret. Time	Area	Height	Conc.	Unit	Mark	Name
1	4.239	330481	16151	51.924	mg/L	V	CL
2	11.670	300560	7366	58.955	mg/L		SO4
3	12.742	32945	898	0.000		V	
Total		663986	24415				

Figure S7

IC chromatogram of *C. patentiramea*. IC, ion chromatography.

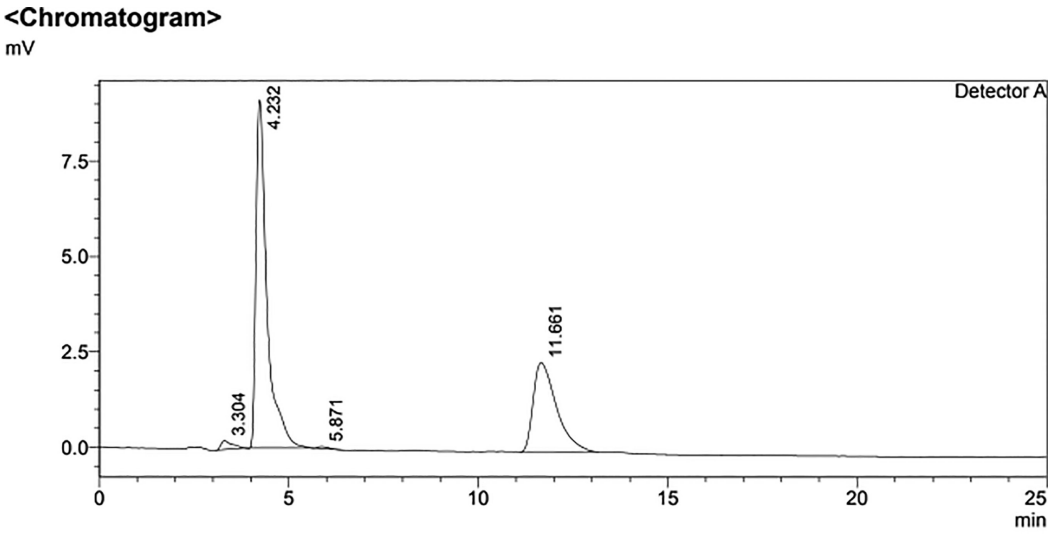

<Peak Table>
Detector A

Peak#	Ret. Time	Area	Height	Conc.	Unit	Mark	Name
1	3.304	4851	231	0.485	mg/L	M	F
2	4.232	186513	9118	29.304	mg/L	M	CL
3	5.871	1083	57	0.268	mg/L	M	NO3
4	11.661	100280	2344	19.670	mg/L		SO4
Total		292727	11750				

Figure S8

IC chromatogram of *L. confervoides*. IC, ion chromatography.

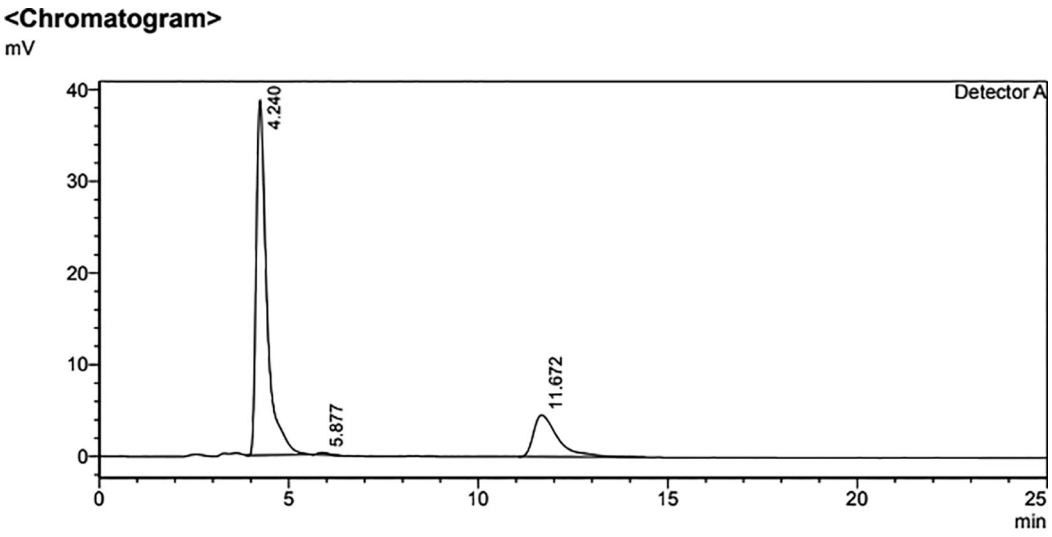

<Peak Table>

Detector A

Peak#	Ret. Time	Area	Height	Conc.	Unit	Mark	Name
1	4.240	761731	38595	119.681	mg/L	M	CL
2	5.877	4853	254	1.200	mg/L	M	NO3
3	11.672	203513	4554	39.919	mg/L		SO4
Total		970097	43403				

Figure S9

IC chromatogram of *C. fastigiatum*. IC, ion chromatography.